Scientia Iranica, Vol. 14, No. 1, pp 46–55

SCIENTIA IRANICA

Modeling of Metal-Mold Interface Resistance in the Al-11.5 wt% Si Alloy Casting Process

S.M.H. Mirbagheri*, M. Shirinparvar[1] and P. Davami[2]

In this investigation, a computational model has been developed, including heat transfer and the effects of the resistance of a metal-mold interface and pressure, for simulation of the solidification process. Simulation of the interface resistance is based on the Zero Thickness Element (ZTE), utilizing the Finite Element Method (FEM). Solid boundary conditions, including contact resistances, have been modified by a pressure gradient in each of the ZTE. The pressure gradient has been modeled, based on experimental data. In order to verify the computational results, an Al-11.5 wt% Si alloy was poured into a permanent mold and the temperature of the interface was measured by a data acquisition system. Then, the effect of metalo-static pressure on overall heat transfer in the interface resistance was modeled. Comparison between the experimental and simulation results during the solidification process shows a good consistency, which confirms the accuracy of the model for the effects of interface resistance on solidification time.

INTRODUCTION

It is demonstrated that when molten metal is poured into a mold cavity, due to surface tension, surface oxidation and mold roughness, there is not only compact contact at the metal-mold interface, but also a contact resistance. Once the cooling process begins, a solid skin develops. Due to contraction of the solid cast and heat expansion of the mold, a gap will be formed between the solidified skin and the mold wall [1]. On the other hand, due to the decomposition of sand binders or evaporation of the refractory coating moisture, gas will fill the gap (gas gap). As a result of this gas gap, the mechanism of heat transfer at the interface becomes pure convection during formation of the solidified skin (not during solidification time). Therefore, gas gap has influence over the temperature distribution of liquid metal in the mold cavity. To predict the heat conduction of a casting process accurately, it is necessary to consider the effect of gas gap and contact resistance on the simulation. Some researchers [2,3] have used a quasi thin element model and coincident nodes technique, based on the FEM at the solid boundary. However, in the thin element model, the size of the gas gap and its variation during the process of solidification, must be known. Also, due to the large aspect ratio of the thin element, error will increase drastically. Moreover, in coincident nodes techniques, element properties are not satisfied and, consequently, the physics of the problem will be changed.

Contact resistance, gas gap formation and pressure are fundamental factors in the solidification rate and their effects on casting are substantial [3,4]. A 10-seconds delay in the formation of the gas gap may cause 10 percent decrease in the solidification time [5]. However, increasing metalo-static pressure could reduce the solidification time. This means that, considering contact resistance, gas gap and pressure are very essential in predicting the solidification time correctly. Therefore, in the present work, in addition to simulating metal-mold heat resistance by the ZTE method, the effect of pressure was also modeled, based on the experimental data, by utilizing an overall heat transfer.

METAL-MOLD INTERFACE RESISTANCE

Heat transfer at the metal-mold interface is very much dependent on the type of surface contact and the media

*. *Corresponding Author, Department of Mining and Metallurgical Engineering, Amirkabir University of Technology, P.O. Box 15875-4413, Tehran, I.R. Iran.*

1. *Quality Management, Esfahan Steel Co., 45 Km Zobahan Freeway, Esfahan, I.R. Iran.*
2. *Department of Materials Science and Engineering, Sharif University of Technology, P.O. Box 11365-9466, Tehran, I.R. Iran.*

between it. Surface contact of the metal-mold interface may be treated in one of the following ways (Figure 1):

i) Without contact resistance,

ii) With contact resistance,

iii) Contact with a thin layer of gas as a media .

Complete contact occurs when the surfaces are under high pressure and of high polishing quality. However, apparent contact occurs when the surfaces are not in complete contact, which is usually due to roughness or coating of the mold and low pressure. This resistance exists until a thick solid skin is formed. In this case, heat is transferred through the spread contact point and the gas layer. Gas gap occurs when solid skin is not deformed under metalo-static or external pressure. Due to contraction of the formed metal skin and expansion of the surrounding model surface, heat is transferred mostly through the layer of gas at the interface.

In general, heat is transferred through the gas gap at the interface by means of convection, radiation and gas conduction. Figure 2 demonstrates the condition of the heat transfer at the interface [6].

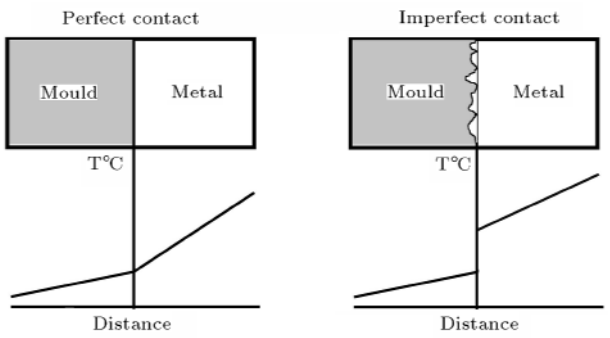

Figure 1. Schematic diagram of metal-mold interface and temperature distribution.

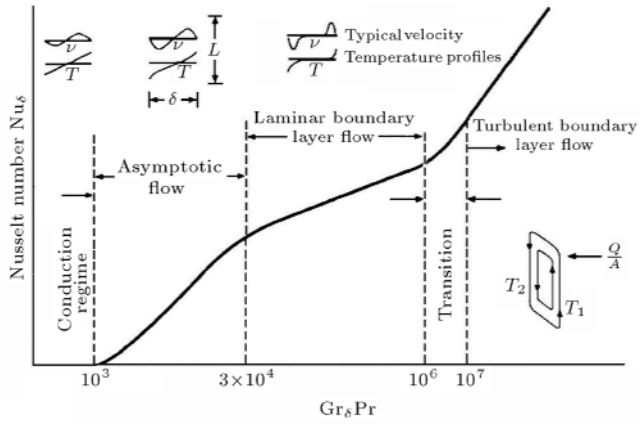

Figure 2. Schematic diagram of the vertical convection layer and flow regime.

The Grashof number (Gr) is one of the parameters, which must be the same in two free convecting systems for them to be dynamically similar. It is defined as follows:

$$\mathrm{Gr} = \frac{g\beta\Delta T d^3}{\upsilon^2}, \tag{1}$$

where g is gravity, β is the thermal expansion coefficient, ΔT is the gap temperature difference, d is the length scale and υ is the kinematics viscosity. So, when $Gr \geq 1$ the viscous force is negligible compared with the buoyancy force and inertia. Also, the inertial forces are negligible. For $Gr \leq 1$, convection occurs when the Rayleigh (Ra) number is more than 1700:

$$\mathrm{Ra} = \frac{g\beta\Delta T d^3}{\upsilon\alpha} = \mathrm{Gr}\,\mathrm{Pr}, \tag{2}$$

where Pr is the Prandtl number and is defined as follows:

$$\mathrm{Pr} = \frac{\upsilon}{\alpha} = \frac{C_P\mu}{k_g},$$

where C_P is the mass heat capacity of gas, k_g is the thermal conductivity of gas, α is the thermal diffusivity and μ is the dynamic viscosity. The Nusselt (Nu) number gives the ratio of actual heat transferred between two parallel plates (gap) at different temperatures by a moving fluid to the heat transfer that would occur by conduction. It is defined by:

$$\mathrm{Nu} = \frac{hd}{k_g}, \tag{3}$$

where h is heat transfer coefficient. As shown in Figure 2, mechanisms of heat transfer at the gap (between the mold and the solid skin) are divided into four regimes [6]:

i) Conduction regime for $\mathrm{Ra} < 1000$,

ii) Asymptotic flow regime for $1000 \leq \mathrm{Ra} < 10000$,

iii) Laminar flow regime $10^4 \leq \mathrm{Ra} < 10^6$,

iv) Transition flow regime $10^6 \leq \mathrm{Ra} < 10^7$,

v) Turbulent flow regime for $\mathrm{Ra} \geq 10^7$.

Holman believes that a high percentage of heat transfer occurs via gas conduction and radiation depending on gap morphology, according to the curve of Figure 2 [6].

It is also possible to define the temperature profile of the metal-mold interface using the Knudsen number (Kn). The small value of the mean free path, (λ), [6] compared with the size of gas gap, (d), confirms that the temperature profile at the interface of casting can always be assumed linear and continuous [7]:

$$\mathrm{Kn} = \frac{\lambda}{d}. \tag{4}$$

However, Fourier's law of heat transfer can be used at the interface. To calculate the overall heat transfer coefficient at the interface, it can be assumed that the media of the interface is a layer of gas with thickness d.

$$h_g = \frac{k}{d}, \tag{5}$$

$$h_t = \frac{q^{\bullet}}{A(T_{ic} \quad T_{is})}, \tag{6}$$

where A is interface area, $q^{\bullet}$ is heat flux through the interface and T_{ic} and T_{is} are casting and mold temperature, respectively. Therefore, contact between casting and mold is never perfect (quasi-contact) and could construct an interface resistance between them. Assume h_g is the heat transfer coefficient, due to the quasi-contact resistance, based on the algorithm of [5]. According to symbols in Figure 3, the rate of heat passed from cast (point 2) to mold (point 1) through the gas layer, d, can be written as:

$$Q = k_B \Delta x \Delta y \left(\frac{T_{me} \quad T_{sk}}{0.5\Delta x} \right), \tag{7}$$

$$Q = h_g \Delta x \Delta y \left(T_{sk} \quad T_{mo} \right), \tag{8}$$

$$Q = k_A \Delta x \Delta y \left(\frac{T_{mo} \quad T_0}{0.5\Delta x} \right). \tag{9}$$

This gives:

$$T_{me} \quad T_0 = Q \left(\frac{1}{2k_A} + \frac{1}{h_g \Delta x} + \frac{1}{2k_B} \right) / \Delta y, \tag{10}$$

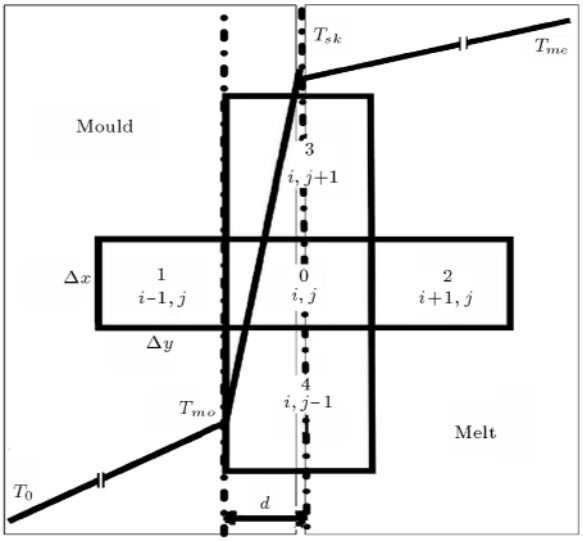

Figure 3. Schematic of discretization of the metal-mold interface. Temperature subscripts are: me = metal liquid, sk = solidified skin, mo = mold.

where k_B and k_A are thermal conductivity coefficients of solidified skin and mold, respectively. Temperatures T_{me}, T_{sk}, T_{mo}, T_0, and other variables are defined in the nomenclature. The overall heat transfer coefficient, h_t, from point '1' to point '0', is defined by:

$$h_t \Delta x = X_A k_A,$$

$$X_A = \frac{2k_B h_g \Delta x}{h_g \Delta x (k_A + k_B) + 2k_A k_B}, \tag{11}$$

where X fraction is the thermal resistance coefficient for each node from the mold-metal interface. The corrective coefficient for the interface nodes can be written as follows:

$$X_{i \quad 1,j} = \frac{2k_{i \quad 1,j} h_g \Delta x}{h_g \Delta x (k_{i \quad 1,j} + k_{i,j}) + 2k_{i \quad 1,j} k_{i,j}}. \tag{12}$$

Also, by considering the heat balances of point '0':

$$\Delta t \left[X_{i \ 1,j} k_{i,j} (T_{i \ 1,j} \quad T_{i,j}) + k_{i,j \ 1} \frac{\Delta x (T_{i,j \ 1} \quad T_{i,j})}{\Delta x \Delta y} \right.$$

$$\left. + k_{i+1,j} \frac{\Delta x (T_{i+1,j} \quad T_{i,j})}{\Delta x \Delta y} + k_{i,j+1} \frac{\Delta x (T_{i,j+1} \quad T_{i,j})}{\Delta x \Delta y} \right]$$

$$= C_{P_{i,j}} \rho_{i,j} (T_{i,j}^{n+1} \quad T_{i,j}). \tag{13}$$

Equations 12 and 13 are discretization forms of Equation 11 and subscripts i and j indicate the x and y directions. Variables in Equations 12 and 13 are defined as before. It is possible that h_t is modeled experimentally by using some thermocouples in the outside metal-mold interface and by substituting the acquired data into Equations 13.

To predict the position of the metal-mold interface and rate of solidification, a fixed value of h_t can be considered. However, it is clear that this assumption is not accurate enough and the value of h_t varies with time and metallurgical parameters. Figure 4 represents a variation of h_t with time for a typical casting process [8]. It is observed that the heat transfer coefficient suddenly increases as the process of pouring the melt begins. As melt convection decreases, the heat transfer coefficient also decreases, gradually reaches a fixed value and remains constant until a solid skin is formed. After this stage, depending on the geometry of the mold and cast, three possibilities may occur, as shown in Figure 4:

1. Decrease in heat transfer coefficient, due to formation of a gas gap;
2. Heat transfer coefficient remains constant; this usually happens at the bottom of the metal-mold interface;
3. Increase in heat transfer coefficient, due to expansion of the mold core, as well as contraction of the cast part.

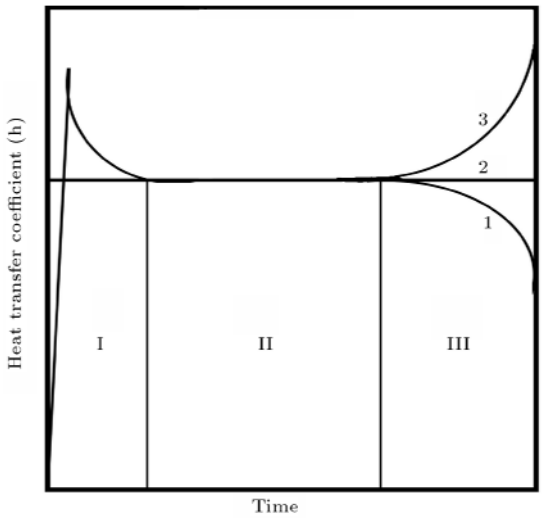

Figure 4. Schematic diagram of the heat transfer coefficient with time.

GOVERNING EQUATIONS

The heat transfer equation may be written as [7]:

$$\rho C_P \frac{\partial T}{\partial t} = \nabla . q + S^{\bullet},$$

$$q = q_x \hat{i} + q_y \hat{j} + q_z \hat{k},$$

$$q_x = k\frac{\partial T}{\partial x}, \quad q_y = k\frac{\partial T}{\partial y}, \quad q_z = k\frac{\partial T}{\partial z}, \tag{14}$$

where term q is the sum of the heat fluxes. The heat source term in Equation 14 can be obtained, as follows:

$$S^{\bullet} = \rho \Delta H_m \frac{\partial f_S}{\partial t}, \tag{15}$$

$$\frac{\partial f_S}{\partial t} = \frac{\partial f_S}{\partial T}\frac{\partial T}{\partial t}. \tag{16}$$

Variables are defined in the nomenclature. The solid fraction in the mushy zone, with assumption partial-mixing in the liquid and no diffusion in the solid, is estimated by Equation 17 [9,10]:

$$C_S = k_E C_L (1 - f_S)^{k_E - 1}, \tag{17}$$

$$\frac{C_S}{k_E C_L} = \frac{T_m - T}{T_m - T_L}, \tag{18}$$

where C_S is the solid composition at the solid-liquid interface, C_L is liquid composition, f_s the solid fraction and k_E the equivalent partition coefficient (between 0 and 1). Also, T_L is the liquidus temperature corresponding to liquid composition C_L and k_E. T_m is the temperature of the melting point. The equivalent distribution coefficient, k_E, is defined by [1,9]:

$$k_E = \frac{k_\bullet}{k_\bullet + (1 - k_\bullet)\exp(\frac{\delta R}{D_L})}, \tag{19}$$

where $k_\bullet$ is the partition coefficient between solid and liquid, δ is the thickness of the segregation layer at the solid-liquid interface, D_L is the liquid diffusion coefficient and R is solidification (growth) rate [9]. Then, substituting Equation 18 into Equation 17 yields:

$$f_S = 1 - \left(\frac{T_m - T}{T_m - T_L}\right)^{\left(\frac{1}{k_E - 1}\right)}. \tag{20}$$

And, substituting Equation 20 into Equation 16 gives:

$$\frac{\partial f_S}{\partial t} = \frac{1}{(T_m - T_L)(k_E - 1)}\left(\frac{T_m - T}{T_m - T_L}\right)^{\left(\frac{2 - k_E}{k_E - 1}\right)}\frac{\partial T}{\partial t}. \tag{21}$$

Variables of Equation 4 are defined as before. The release of the latent heat between liquidus and solidus temperature is calculated by substituting Equation 21 into Equation 15. To implement this equation, the following assumptions are made:

1. The physical properties of the liquid, solid and mold are assumed constant in the solidification process. However, in the mushy zone, they are, as follows:

$$k_M = f_L k_L + f_S k_S,$$

$$\rho_M = f_L \rho_L + f_S \rho_S.$$

2. The overall heat transfer coefficient, h_t, including transferred heat, due to contact points, gas gap and radiation ($h_t = h_c + h_g + h_r$), are considered.

Consider the physical domain of (Ω), with boundaries of (Γ_1), (Γ_2) and metal-mold interface (Γ_3). The boundary condition is [11,12]:

$T(r,t) = \hat{T}(r,t)$ at Γ_1 Dirichlet B.C.

and:

$k\nabla T.n = q = h(T - T_0)$ at Γ_2 Neuman B.C.

The initial condition is:

$T(r,0) = T_0$ in the mold,

$T(r,0) = T_{\text{Pour}}$ in the cast.

FEM Modeling

Due to the symmetrical properties of the cylindrical geometry, the 3D heat transfer equation reduces to a 2D equation, where, through implementation, the

Finite Element Method (FEM) formation may be written as [11]:

$$[\mathbf{C}]\{\mathbf{T}^{\bullet}\} + [\mathbf{K}]\{\mathbf{T}\} = \{\mathbf{F}\}, \tag{22}$$

where $\{\mathbf{T}\}$ and $\{\mathbf{T}^{\bullet}\}$ are vectors of the temperatures and the temperature gradients, respectively. Also, stiffness matrix $[\mathbf{K}]$, capacitance matrix $[\mathbf{C}]$ and force vector $\{\mathbf{F}\}$, are defined, respectively, as:

$$K_{i,j} = \int_{\Omega} \nabla N_j (K \nabla N_j) d\Omega + \int_{2} h_b N_i N_j d\ _2, \tag{23}$$

$$C_{i,j} = \int_{\Omega} \rho C_P N_i N_j d\Omega, \tag{24}$$

$$F_i = \int_{2} (q \quad h_b T_0) N_i d\ _2, \tag{25}$$

where, N_i and N_j are elements shape functions, whose details are explained in [11,12]. T is the nodal temperature vector, h_b is the boundary heat transfer coefficient and T_0 is the ambient temperature. It is important to note that heat transfer at the central line of the cylinder has been neglected and convection takes place between the cylinder and the surroundings. In this work, the overall heat transfer coefficient has been modeled experimentally, which includes the effects of conduction, convection, radiation and contact points (see the following sections).

Due to solving the transient part of Equation 14, the Finite Difference Method (FDM) technique is used, using the θ method, via the time stepping algorithm:

$$[C + \theta K \Delta t]\{C\}_{i+1} = [C \quad (1 \quad \theta) K \Delta t]\{C\}_i + [(1 \quad \theta) F_i + \theta F_{i+1}]\Delta t. \tag{26}$$

This method includes forward, central and backward difference schemes, with values of $\theta = 0.5$ and 1, respectively [11].

Modeling of Zero Thickness Elements at Interface

In the casting simulation problem, correct modeling of the interface resistance plays an important role in the accuracy of the results. Ignoring interface resistance in the solidification process could generate an error between 50-100% in the solidification time [12-14]. Most solidification simulation codes do not have the substantially imposed effects of the gas gap in their algorithms and some of them assume that the neighboring elements of cast and mold have full contact. In this simulation, a Zero Thickness Element (ZTE) is introduced for implementation of the interface resistance [12]. Figure 5 represents such a model at an interface; nodes 3, 4, 5 and 6 are ZTE nodes, connecting elements A and B at the cast and the mold, respectively. Also, Figure 5 shows the node numbers configuration of the ZTE, with the neighboring elements.

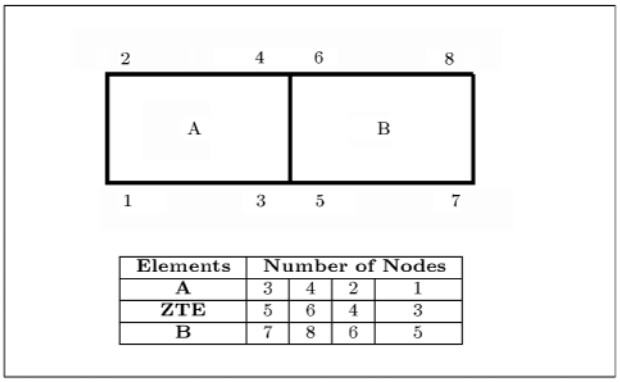

Elements	Number of Nodes			
A	3	4	2	1
ZTE	5	6	4	3
B	7	8	6	5

Figure 5. Node numbers configuration of ZTE with the neighboring elements.

Heat is transferred at the interface between elements A and B, by convection, with an overall heat transfer coefficient, h_t, through ZTE. The shape function for ZTE, considering the local coordinate system of ξ and η, may be written as:

$$N_1^{\mathrm{ZET}} = 0.5(1 \quad \xi), \qquad N_2^{\mathrm{ZET}} = 0.5(1 + \xi). \tag{27}$$

The stiffness matrix for this element is defined as:

$$K_{i,j}^{e} = \int_{3} h N_i N_j d\ _3, \tag{28}$$

where $_3$ represents the metal-mold boundary and h is the overall heat transfer at the interface. The overall heat transfer coefficient may be defined experimentally or calculated mathematically. Finally, Equation 28 may be written as:

$$K_{i,j}^{e} = \int_{1}^{1} h N_i N_j |J| n d\xi, \tag{29}$$

where n is the unit normal to the surface of the integration and should be selected properly, based on the physics of the problem.

EXPERIMENTAL SET-UP

The apparatus shown in Figure 6a was designed to measure the temperature and calculate the overall heat transfer coefficient (h_t). The mold was a Grey Cast Iron cylinder with an isolated bottom. The samples were cast with Al-11.5 wt% Si alloy. In this experiment, one thermocouple (type K) is inserted into the melt

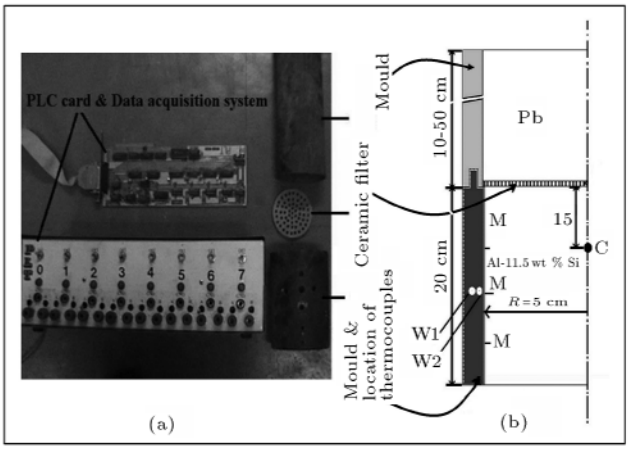

Figure 6. a) Installation of PLC card and the data acquisition system on the mold; b) Schematics of geometry and dimensions of cylindrical mold.

and one thermocouple attached to the metal-mold interface, in order to show the temperatures of the metal and the interface, respectively (Figure 6b).

Temperature data were acquired utilizing a PLC-32 bit card of 10 kHz, 12 channels and HG818L-advantech. Each experiment was duplicated for reliability purposes.

As demonstrated in Figure 6, a ceramic filter was placed between two parts of the mold and, then, molten Pb filled the upper-part of the mold, in order to measure the effect of the pressure on the h_t coefficient. The height of the Pb in the mold varied between 10-50 cm. In order to achieve higher pressure, Pb metal was used in the mold. Because metal-static pressure of Pb is higher, the Al alloy is the same as the height.

Interface and mold wall temperatures were measured experimentally at different pressures (Figure 7).

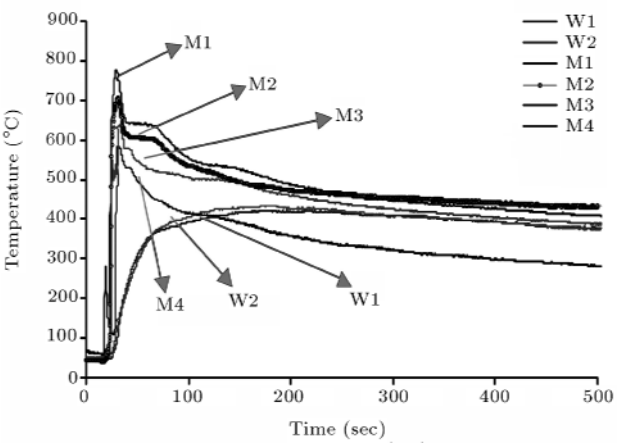

Figure 7. Measuring the metalo-static pressure effect on the $T \quad t$ curve during solidification process by data acquisition system, M1: $H_{Pb} = 10$, M2: $H_{Pb} = 20$; M3: $H_{Pb} = 40$; M4: $H_{Pb} = 50$ cm.

RESULTS AND DISCUSSION

In this investigation, a new experimental model has been developed for predicting the effective pressure gradient on the overall heat transfer coefficient, h_t, based on experimental data. As shown in Figure 8, it is clear that the head of the metalo-static pressure or effective height, $H_{\text{eff.}}$, could alter the h_t coefficient. Therefore, an equivalent h_t of $H_{\text{eff.}}$ can be obtained, corresponding to the present mathematical model, as follows:

$$h_t = H_\bullet \lfloor 1 + (a)\exp(\quad b(\Delta P)^n) \rfloor ,$$

$$\Delta P = \rho g H_{\text{eff}}, \tag{30}$$

where $a = 1.55$, $b = 10^{\ 5}$ and $n = 3$ are equation coefficients, after best fitting by the S-PLUS 200 mathematical software. $H_{\text{eff.}} = H_\bullet \quad (L^2/2L_\bullet)$ was defined in Figure 8, $H_\bullet$ = sprue height, L = distance between the cavity inlet and the top of the mold cavity and $2L_\bullet$ = mold cavity height. Figure 9 shows the effect of gradient pressure on the solidification time.

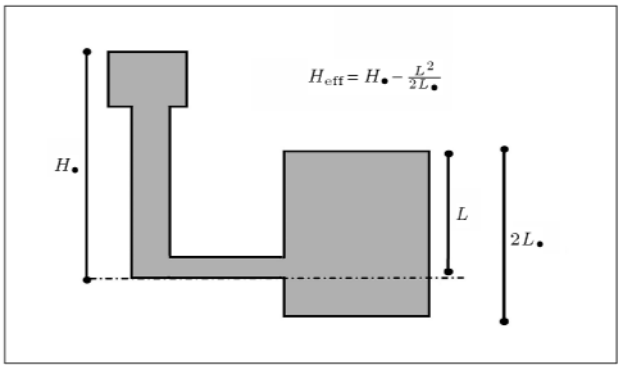

Figure 8. Schematic of calculating the effective height in the gating system design; $H_\bullet$: Sprue height, L: Distance between the cavity inlet and the top of the mold and $2L_\bullet$: Mold cavity height.

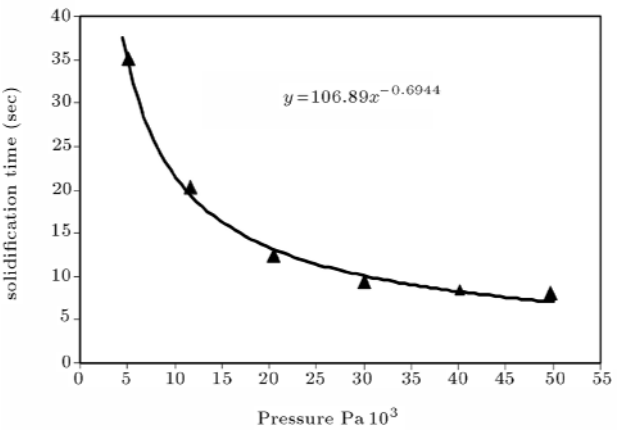

Figure 9. Effect of the metalo-static pressure on the solidification time.

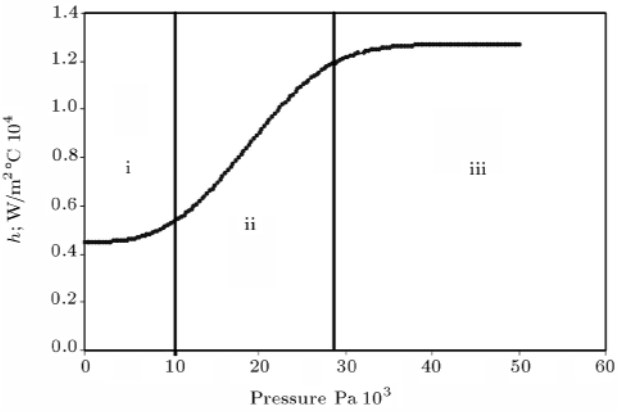

Figure 10. Modeling of the heat transfer coefficient (h) versus the metalo-static pressure; i: Solid skin formation, ii: Solid skin deformation and iii: Solid skin growth.

In this figure, once temperature of the thermocouple in the cylinder center goes below T_S, solidification times are registered and saved. Figure 10 shows the effect of metalo-static pressure on h. For pressures less than 100-120 KPa, curve $P \quad h$, in Figure 10, is divided into 3 different zones. Zone i indicates solid skin formation, Zone ii indicates solid skin deformation (increasing contact surface) and Zone iii indicates solid skin growth or saturated zone. It is clear that the heat transfer coefficient increases sharply into Zone ii and the mushy skin penetrates into the roughness of the mold wall, leading to perfect contact and increased h_t. Therefore, as shown in Figure 9, solidification time will be reduced.

A simulation of temperature distribution was carried out by using the new model (h_t) at each time step. Due to mold symmetry, only half of the mold was simulated. Figure 11 shows simulation of the temperature distribution during the solidification process of the Al-11.5 wt% Si alloy, based on data presented in Table 1.

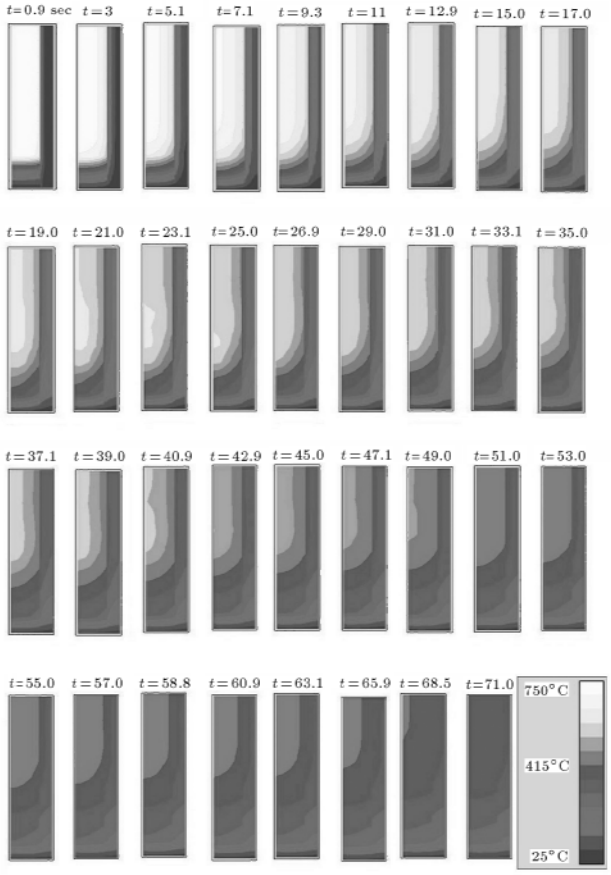

Figure 11a. Simulation of the effect of contact resistance on the temperature distribution for Al-11.5 wt% Si with minimum metalo-static pressure ($H_{Pb} = 0$) by the ZTE model (solidification time = 68.51).

Figures 11a and 11b show the results of temperature distribution simulation, by adding to the ZTE model, with minimum (Pb melt head; $H_{Pb} = 0$ cm) and maximum (Pb melt head; $H_{Pb} = 50$ cm) contact resistance, respectively. However, Figure 11c shows the

Table 1. Properties of mold and metal for simulation of heat transfer in the casting process.

Property	Mold	Metal
Material: (% wt)	C=2.3, Si=3.2, Mn=0.75, S=⟨ P 0.01	Si=11.5, Fe=0.05, Al=bal
Pouring temperature (°C)	1350 ± 5	775 ± 5
Thermal conductivity (J/sec. m°C)	$k_L = 0.069$, $k_S = 0.07$, $k_{\text{Chalk}} = 0.001$	$k_L = 0.42$, $k_S = 0.42$
Heat of fusion (J/kg)	–	$\Delta H_f = 0.4186$
Specific heat (J/k°Cg)	$C_p^l = 9.63\ 10^4$, $C_p^S = 8.79\ 10^4$, $C_p^{\text{Chalk}} = 9.63\ 10^4$	$C_p^l = 1.13\ 10^3$, $C_p^S = 1.09\ 10^3$
Density (kg./m^3)	$\rho_S = 7300$, $\rho_{\text{Chalk}} = 1610$,	$\rho_L = 2500$, $\rho_S = 2600$
Transformation temperature (°C)	–	$T_L = 615 \pm 1$, $T_S = 572 \pm 1$
Time step (sec)	0.25	
Number elements	$N = 8746552$	
CPU time for Pentium IX 600 (h)	38	
Boundary conditions	Wall: Free slip	

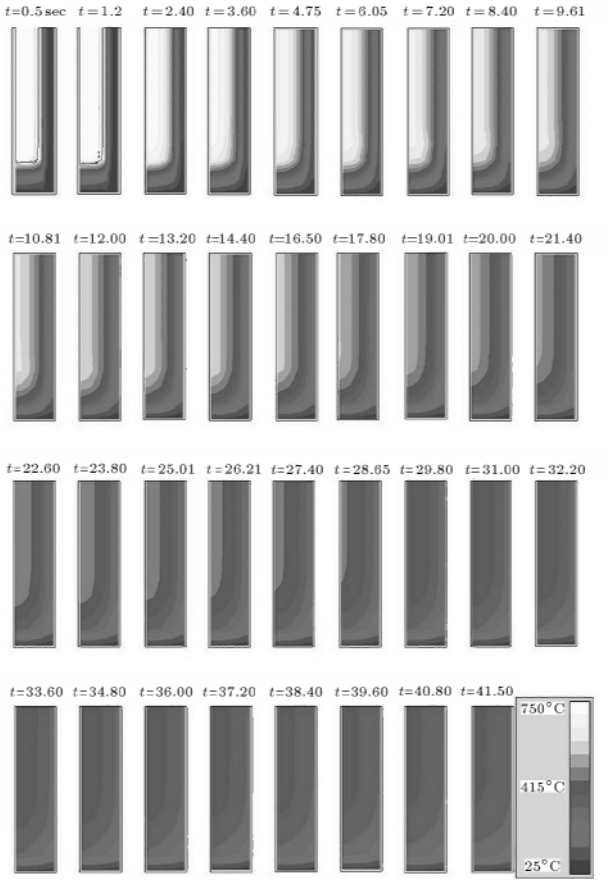

Figure 11b. Simulation of effect of contact resistance on the temperature distribution for Al-11.5 wt% Si with maximum metalo-static pressure ($H_{Pb} = 50$) by the ZTE model (solidification time = 40.80).

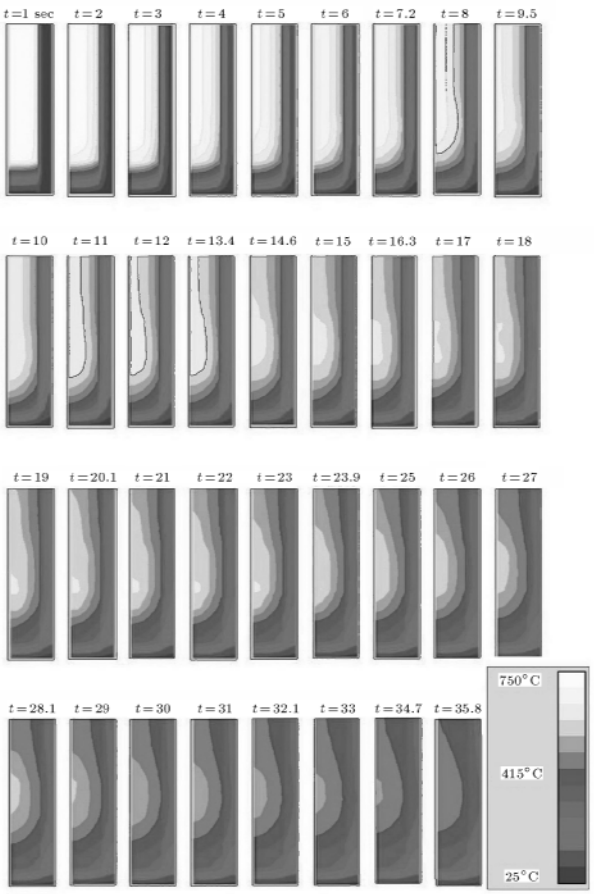

Figure 11c. Simulation of effect of contact resistance on the temperature distribution for Al-11.5 wt% Si with minimum metalo-static pressure ($H_{Pb} = 0$) without the ZTE model (solidification time = 36.02).

results of temperature distribution simulation without the ZTE model in the case of minimum pressure (Pb melt head; H_{Pb}=0 cm). It is evident that the interface effect considered in the present numerical model has resulted in a solidification time and temperature distribution that approaches the experimental result.

The effect of contact resistance on the temperature variation with time at a fixed point in the center of the cylinder can be seen in Figure 12. It is seen that, without consideration of the interface resistance effect (gas gap) in low metalo-static pressure ($H_{Pb} = 0$), an error of $100 \times (68.51 \quad 36.02)/68.51 = 47.5\%$ in solidification time is introduced. However, the error will be $100 \times (40.08 \quad 28.86)/40.08 = 28\%$ for high metalo-static pressure.

The comparison between the experimental and simulation results shows a good level of consistency, which confirms the accuracy of the model for predicting heat resistance at the interface of a metal-mold.

CONCLUSION

i) The heat transfer code developed in this research simulates the effect of interface resistance (gas gap) based on the Zero Thickness Element method. It could predict temperature distribution in the metal, as well as in the mold, throughout the

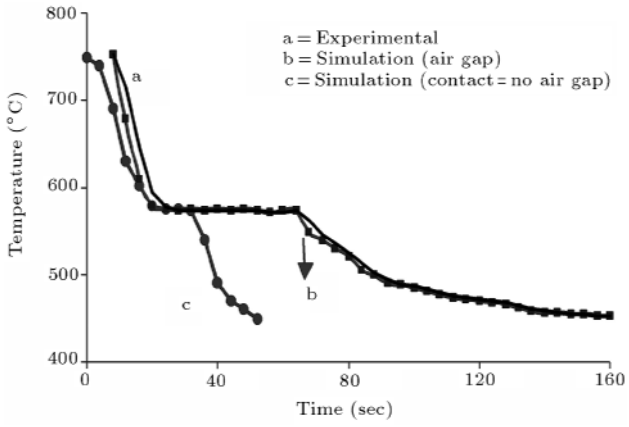

Figure 12. The effect of contact resistance (high interface resistance) and gas gap on the temperature variation with time at a fixed point in the center of the cylinder (point C in Figure 6) for Al-wt%11 Si alloy.

solidification period, utilizing the modeling effect of pressure on interface resistance;

ii) In low-pressure casting, heat transfer coefficient increases as a power law function, when metalostatic pressure could penetrate through the mushy solid skin into the roughness of the mold wall;

iii) The comparison between experimental results, obtained from the data acquisition system and the simulation results, verifies the validity of the model predictions. It is worth mentioning that consideration of the interface resistance effect reduces the solidification time by 40-50% and modifies temperature distribution in the system dramatically.

ACKNOWLEDGMENT

The authors are grateful for the research support of the Department of Materials Science at Imperial College, London and of Sharif University, Amirkabir University and the Esfahan Steel Making Co. in Iran.

NOMENCLATURE

A	interface area in Equation 6
a	constant of Equation 30
b	constant of Equation 30
$[\mathbf{C}]$	capacitance matrix in Equations 22 and 24
$C_\circ$	initial alloy content
C_L	concentration of alloying element in liquid
C_P	heat capacity
C_S	concentration of alloying element in solid
D_L	diffusion coefficient in liquid
d	thickness of gas gap
e	acronym element
$[\mathbf{F}]$	force vector in Equations 22 and 25
f_S	solid fraction
f_L	liquid fraction
g	gravity acceleration
Gr	Grashof number
$H_\bullet$	height of sprue filled by the Al alloy
H_{Pb}	height of sprue filled by the Pb
H_{eff}	effective height in Figure 8
h	heat transfer coefficient
h_g	heat transfer coefficient of gap
h_t	overall heat transfer coefficient
J	Jacobian matrix in Equation 29
$[\mathbf{K}]$	stiffness matrix in Equations 22 and 23
Kn	Knudsen number
k	thermal conductivity
$k_\bullet$	distribution coefficient
k_A	thermal conductivity coefficient of mold
k_B	thermal conductivity coefficient of solidified skin
k_E	equivalent distribution coefficient
k_g	thermal conductivity of gap
k_L	thermal conductivity of liquid
k_M	thermal conductivity of mushy zone liquid
k_S	thermal conductivity of solid
L	distance between cavity inlet and top of mold cavity
$L_\bullet$	half of mold cavity height
$N_1^{\mathrm{ZTE}}, N_2^{\mathrm{ZTE}}$	shape functions of zero thickness element
N_i, N_j	shape functions of general elements
Nu	Nusselt number
n	normal vector of interface in Equation 29
P	pressure
Pr	Prandtl number
Q	rate of heat passed through gas layer d
q	sum of heat flux on 3D space
$q^\bullet$	heat flux through the interface
R	growth rate of solid-liquid interface
Ra	Rayleigh number
Re	Reynolds number
$S^\bullet$	heat source term
$\{\mathbf{T}\}$	temperature vector
$\{\mathbf{T}^\bullet\}$	temperature rate vector
T	temperature
$T_\circ$	ambient temperature
T_{ic}	cast temperature at interface
T_{is}	mold temperature at interface
T_L	liquidus temperature
T_m	melting point
T_{me}	melt temperature
T_{mo}	mold temperature
T_S	solidus temperature
T_{sk}	solid skin temperature at interface
X	thermal resistance coefficient in Equations 6 to 19

Greek Alphabet

$_1$	boundary with Dirichlet condition

$_2$	boundary with Neumann condition
$_3$	metal-mold boundary
ΔH_m	latent heat of solidification
Δt	time step
$\Delta x, \Delta y$	elements dimensions
Ω	domain
Ω_1	domain between $_2$ and $_3$
Ω_2	domain between $_1$ and $_3$
α	thermal diffusivity
β	thermal expansion
δ	supersaturate layer at solid-liquid interface
η, ξ	local coordinate system
θ	FDM methods coefficient
λ	mean free path in gap
μ	dynamic viscosity
ρ_L	density of liquid
ρ_M	density of mushy zone
ρ_S	density of solid
υ	kinematics viscosity

REFERENCES

1. Mukherjee, P.C., *Fundamentals of Metal Casting Technology*, Oxford & IBH publishing Co. India, Chap: 4 (1979).
2. Santos, C.A., Quaresma, J.M.V. and Garcia, A. "Determination of transient interfacial heat transfer coefficients in chill mold castings", *Journal of Alloys and Compounds*, **319**, pp 174-186 (2001).
3. Li, K., Cheng, M. and Change, E. "Effect of pressure on the feeding behavior of A356 alloys in low-pressure casting", *AFS Transaction*, **01**(26), pp 566-580, (2001).
4. Loulou, T. Artyukhin, E.A., and Bardon, J.P. "Estimation of thermal contact resistance during the first stage on metal solidification process", *Int. J. Heat and Mass Transfer*, **42**, p 2119 (1999).
5. Isaac, J., Reddy, G.P. and Sharma, G.K. "Numerical simulation of solidification of castings in metallic molds", *AFS Transaction*, **93**(14), pp 123-132 (1985).
6. Holman, J.P., *Heat Transfer*, McGraw-Hill, New York, USA (1981).
7. Song, S., Yovanovich, M.M. and Goodman, F.O. "Thermal gap conductance of conforming surfaces in contact", *Trans. ASME, J. Heat Transfer*, **115**(3), pp 533-540 (1993).
8. Sharma, G.K. and Krishnan, M. "A model of the interfacial heat-transfer coefficient during solidification of an aluminum alloy", *AFS Transaction*, **91**, p 429 (1983).
9. Siqueira, C.A. Cheung, C. and Garcia, N. "The columnar to equiaxed transition during solidification of Pb-Sn alloy", *J. of Alloys and Compounds*, **2**(351), pp 126-134 (2003).
10. Narayan Prabhu, K. and Ravishankar, B.N. "Effect of modification melt treatment on casting/chill interfacial heat transfer and electrical conductivity of Al-13%Si alloy", *Materials Science and Engineering*, **A360**, pp 293-298, (2003).
11. Stasa, F.L., *Applied Finite Element Analysis for Engineering*, CBS publication Japan Ltd. (1985).
12. Shrinparvar, M. "Simulation of heat transfers in metal-mold interface", M.S thesis, Sharif University of Technology, Tehran, Iran (2004).
13. Samonds M., Lewis, R.W. and Morgan K., *Computational Techniques in Heat Transfer*, Pineridge Press, Swansea, U.K. (1985).
14. Tadayon, M.R. and Lewis, R.W. "A model of metal-mold interfacial heat transfer for finite element simulation of gravity die castings", *Cast Metals*, **1**(1), pp 24-29 (1988).